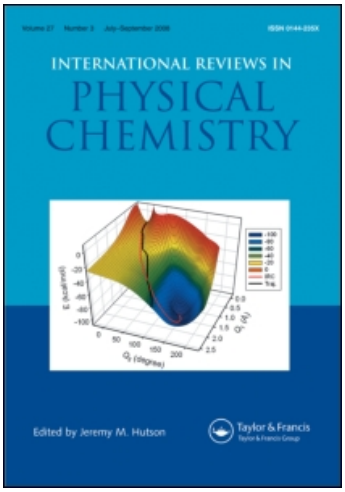

International Reviews in Physical Chemistry
Publication details, including instructions for authors and subscription information:
http://www.informaworld.com/smpp/title~content=t713724383

Location control of electron donors and acceptors in photoinduced charge separation across surfactant interfaces

Larry Kevan[a]
[a] Department of Chemistry, University of Houston, Houston, Texas, USA

To cite this Article Kevan, Larry(1990) 'Location control of electron donors and acceptors in photoinduced charge separation across surfactant interfaces', International Reviews in Physical Chemistry, 9: 4, 307 — 328
To link to this Article: DOI: 10.1080/01442359009353249
URL: http://dx.doi.org/10.1080/01442359009353249

INTERNATIONAL REVIEWS IN PHYSICAL CHEMISTRY, 1990, VOL. 9, NO. 4, 307–328

Location control of electron donors and acceptors in photoinduced charge separation across surfactant interfaces

by LARRY KEVAN
Department of Chemistry,
University of Houston, Houston, Texas 77204, U.S.A.

The efficiency of photoinduced charge separation across surfactant interfaces of micelles and vesicles depends in part on the location of electron donors and acceptors relative to the interface. Achievement and assessment of control of such location by the addition of pendant alkyl chains to donors and acceptors are reviewed. The net photo-ionization efficiency can be measured by electron spin resonance of radical ions in frozen surfactant solutions. Assessment of relative locations of radical ions with respect to a surfactant interface has been achieved by analysis of electron spin-echo modulation with deuterated water at the interface. Alkylmethylviologen electron acceptors are shown to be particularly useful for location control of photo-ionization efficiency in vesicles and less so in micelles. Electron donors investigated for location control include alkylated ruthenium *tris*(bipyridyl) species and alkylphenothiazine sulphonate derivatives. Photo-induced conversion of alkylmethylviologen radical ion to surfactant radicals is shown to enhance the net photo-ionization efficiency. Comparative photo-ionization efficiency results in vesicles, micelles and reverse micelles reveal structural aspects of effective location control by pendant alkyl chains.

1. Introduction

Photoinduced charge separation of photo-ionizable solutes in organized molecular assemblies such as micelles, vesicles, reverse micelles and microemulsions is a currently active area of study with a goal to optimize the storage of light energy (Grätzel 1988). Such a goal is a type of artificial photosynthesis and in many ways parallels natural photosynthesis, in which a chlorophyll solute in a lipid bilayer is photo-ionized, resulting in electron transfer to a chain of electron acceptors which causes net charge separation and ultimate chemical conversion of this stored light energy into chemical energy.

The focus of this review involves the structural aspects that control photoinduced charge separation across surfactant interfaces. Photo-ionization results in a paramagnetic electron acceptor and electron donor, one or both of which may have sufficient lifetime to be detected as such. Transient optical absorption is an important way to detect such intermediates but electron spin resonance (ESR) is specifically useful to detect only paramagnetic intermediates in such charge-separation processes. ESR has the additional advantage that it can be used to probe the surroundings of the paramagnetic species and to answer questions as to the location of the electron donor cation or electron acceptor anion with respect to the surfactant assembly structure and its interface. However, the spectral resolution for magnetic interactions of the paramagnetic species with its surroundings is often quite limited in an ESR spectrum. Important advances in probing the surroundings of electron donor cations and electron acceptor anions in surfactant assemblies have been recently made by exploitation of the increased resolution available from a pulsed ESR technique called

0144–235X/90 $3·00

electron spin-echo modulation (ESEM) (Kevan 1979). For example ESEM can be used to measure the interaction of a paramagnetic species with water at a surfactant assembly interface and more importantly can monitor changes in the extent of that interaction as a function of experimentally controllable variables affecting the structure of the surfactant assembly.

In this summary we shall briefly review the background of ESEM for an understanding of its power when applied to such problems. Then a brief summary of the photo-ionization of solutes in micelles and vesicles and how the efficiency of such can be controlled structurally by modification of the surfactant assembly interface will be given. The main focus of the chapter will be the description and development of location control of electron donors and acceptors with respect to a surfactant assembly interface by adding alkyl chains of variable lengths to such photo-ionizable or photoreducible molecules.

2. ESEM background

In a paramagnetic system an electron spin echo (ESE) is produced in response to a two-pulse sequence in which the first 90° pulse causes focusing of the spin system and after a time τ, during which the spin system dephases, a second 180° pulse causes the initiation of refocusing which after another time τ after the second pulse results in the generation of a burst of microwave energy called an echo. The ESE intensity is measured as a function of the interpulse delay time as shown in figure 1. In solid systems in which the dipolar electron–nuclear hyperfine interaction is *not* averaged out by rapid tumbling of molecules the echo intensity as a function of interpulse time is often modulated as also shown in figure 1. This echo intensity modulation arises from relatively weak electron–nuclear hyperfine interaction to which the paramagnetic spins are exposed as they undergo dephasing and rephasing. An analysis of this modulation gives information about the number and distance of magnetic nuclei surrounding the paramagnetic centre (Kevan 1979).

Since the structure of surfactant assemblies such as micelles and vesicles is complex and rather disordered, it has been found to be most useful to analyse the modulation in such systems in terms of the normalized modulation depth at the first minimum in the modulation period. The absolute modulation depth is shown in figure 1; it is normalized by dividing by the distance from the unmodulated broken curve to the baseline. In the work to be summarized in this review the modulation is always caused by interaction with deuterium nuclei for which the first modulation period is normally detected experimentally. The normalized deuterium modulation depth is a function of both the distance and number of surrounding deuterium nuclei from the paramagnetic species. The detection of deuterium modulation is possible for physically reasonable numbers of deuterium nuclei based on molecular density out to a distance of about 0·6 nm.

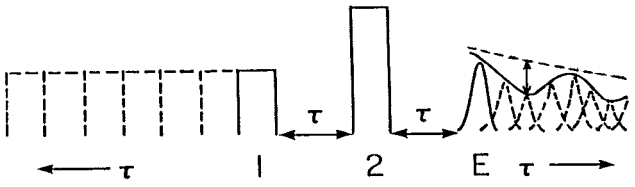

Figure 1. Schematic diagram of a two-pulse ESE experiment where τ is the interpulse time and the echo is E. Variation in τ is shown by the broken lines. The modulation depth is shown by the vertical arrow at the first modulation minimum.

As stated above, the analysis and exploitation of ESEM requires solid systems. Hence the surfactant assemblies must be rapidly frozen in order to make analysis possible. This poses no real limitation because numerous studies have demonstrated that in relatively rapidly frozen aqueous solutions the micellar and vesicular structure is retained. In addition, many ion-solvation studies demonstrate retention of the solvation shell in rapidly frozen aqueous solutions (Kevan 1981). Specific evidence that micellar structure is retained in frozen solutions is based on an increasing variety of experiments which include the following.

(1) The long lifetime of photo-produced tetramethylbenzidine radical cations in micelles but not in bulk solution supports this (Narayana *et al.* 1981).
(2) Analogous photo-ionization trends for molecules embedded in micelles and vesicles are found (Li and Kevan 1983). Since vesicles are considered to be more organized in their interiors than are micelles, this argues that micellar structure is retained in addition to vesicular structure in frozen solutions.
(3) It has also been found that similar aggregation numbers, that is the number of surfactant molecules making up a micelle, are measured in liquid and frozen micellar solutions by luminescent quenching methods (Hashimoto and Thomas 1983).
(4) Micellar structure can also be directly detected in frozen micellar solutions by electron microscopy (Bachman *et al.* 1981).
(5) It has been found that certain countercations such as the tetramethylammonium cation open up the surface structure of an anionic micelle such as sodium dodecylsulphate (SDS) to increase the low concentration of water at the interface. It has been possible to study this effect in both liquid and solid media and the results are similar in both cases (Hiromitsu and Kevan 1986). Thus this argues for retention of micellar structure in the frozen solution.
(6) It has also been possible to use ESEM methods to measure the partition coefficients of alcohols between the micellar interface and the bulk phase in frozen SDS micellar solutions (Baglioni and Kevan 1987). The values are found to agree with values determined by nuclear magnetic resonance or thermochemistry in SDS liquid micellar solutions.
(7) Similar experiments have been carried out to measure the partition coefficients of crown ethers between the micelle interface and the bulk solution; the results by ESEM methods in frozen SDS micellar solutions agree with those measured by other techniques in liquid micellar solutions.

This extensive body of evidence indicates unambiguously that the micellar structure and also the vesicular structure are retained in the frozen solutions; these studies are now described.

3. Solute photo-ionization in micelles and vesicles

The photo-ionization of molecules such as tetramethylbenzidine, chlorophyll and zinc tetraphenylporphyrin in a variety of micellar and vesicular systems has been studied over the last few years by ESR and ESEM methods (Kevan 1988). In general it has been found that the photo-ionization efficiency correlates with stronger interactions between the photo-produced cation and deuterated water at the interface of the surfactant assembly as measured by ESEM methods. A stronger interaction is characterized by deeper deuterium modulation and so correlations have been

investigated between the depth of the deuterium modulation from deuterated water at the interface and the net photo-ionization yield as measured by ESR. Thus it has been concluded that charge separation across surfactant interfaces is enhanced by electron hydration or injection into the water phase at the interface. Of course, if there is a specific electron acceptor present, its location and its chemistry will often control the net photo-ionization. The generalization stated above applies when the electron acceptor is bulk water.

In general, the net charge separation across the surfactant interfaces depends upon the following factors.

(1) The solute location within the micellar or vesicular assembly is a control factor for net charge separation. It is almost always found that the electron donor is asymmetrically located within the surfactant assembly and is relatively near to the interface.
(2) Another control factor is the micelle or vesicle size. In general a smaller size, as controlled by the length of the alkyl chain of the surfactant molecule, leads to higher photo-ionization efficiency although the size cannot be too small.
(3) A major control factor is the interface charge. In frozen systems it is found that a positive interface charge is generally better because it allows the electron to escape across the interface whereas a negative surface or interface charge tends to impede the electron from traversing the interface.
(4) Likewise the interface charge density is a control factor in which a more positive or less negative charge density enhances the photo-ionization efficiency.
(5) The ionic strength of the interface is another control factor. It can be varied by added salts and by specific complexation of counterions by crown ethers. The ionic strength effect depends on the charge of the interface such that increased ionic strength can lead to either greater or lesser photo-ionization efficiency depending on the charge of the interface.
(6) Finally, when a specific molecular electron acceptor is present, the relative locations of the electron donor and acceptor are major control factors for the photo-ionization efficiency. For efficient charge separation the acceptor should be close but not too close or back electron transfer will be too facile.

Figures 2 and 3 show typical structures and dimensions of a micelle and a unilamellar spherical vesicle that will be principally studied as surfactant assemblies in the results to be summarized. Note that surfactant-forming micelles typically have one alkyl chain of 8 to 16 carbons and surfactant-forming vesicles typically have two alkyl chains of 8 to 18 carbons. The table shows the structures of some commonly used surfactants that form micelles and vesicles.

4. Photoreduction of alkylmethylviologens

Methylviologen dication solubilized in SDS micelles at room temperature may be easily photoreduced by ultraviolet light. The formation of the methylviologen monocation is indicated visually by a blue colour and also by an ESR spectrum. Figure 4 shows a resolved spectrum of the methylviologen monocation in which ultraviolet photolysis was carried out in a frozen SDS solution at 77 K. At this temperature the spectrum is one broad line with unresolved hyperfine splitting, but on warming to room temperature the resolved spectrum shown in figure 4 is obtained. The hyperfine

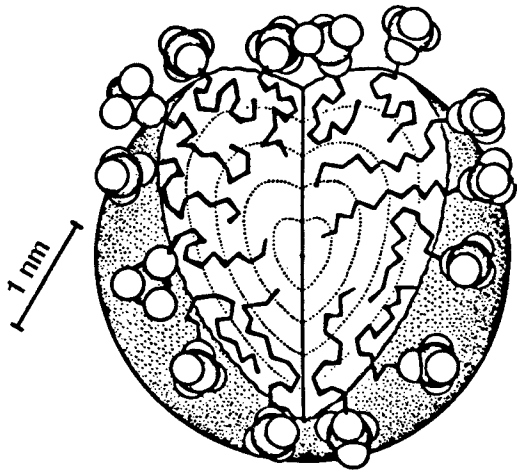

Figure 2. Schematic diagram of a statistical mechanical model of a dodecyl sulphate micelle in water. The micelle diameter is about 4 nm and the sulphate groups cover about 16% of the surface area.

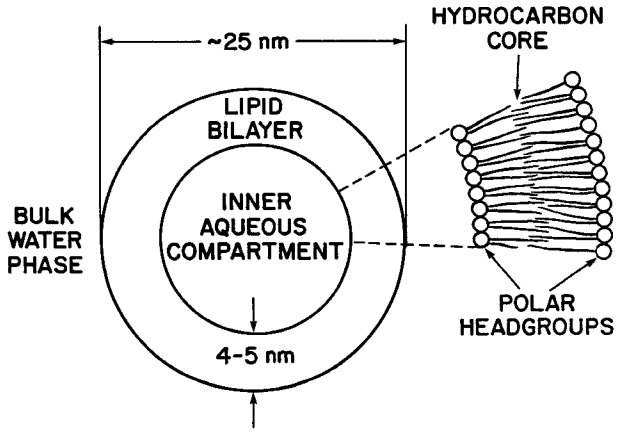

Figure 3. Schematic diagram of a unilamellar vesicle.

Structures of some commonly used surfactants that form micelles and vesicles.

	Micelle formers
Sodium dodecylsulphate (SDS)	$Na^+SO_4^-—C_{12}$
Dodecyltrimethylammonium chloride (DTAC)	$C_{12}—N(CH_3)_3^+\ Cl^-$
Hexakis(ethylene glycol) monododecyl ether	$C_{12}—O—(CHOH—CHOH)_6—H$
	Vesicle formers
Dihexadecylphosphate (DHP)	$(C_{16})_2—POO^-\ H^+$
Dioctadecyldimethylammonium chloride (DODAC)	$(C_{18})_2—N(CH_3)_2^+\ Cl^-$
Dipalmitoylphosphatidylcholine (DPPC)	$(C_{15}COOCH_2)—(C_{15}COOCH)—CH_2OPO_3^-CH_2CH_2N^+(CH_3)_3$

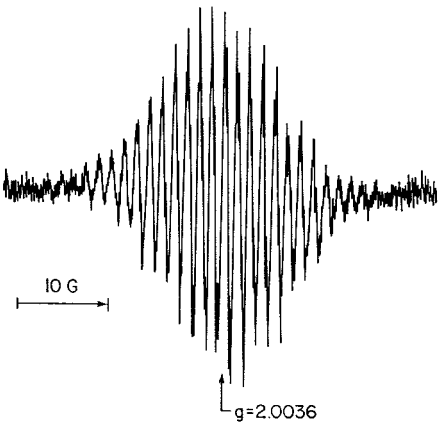

Figure 4. First-derivative room temperature ESR spectrum at the X band of the MV^+ radical cation obtained from 77 K ultraviolet-irradiated frozen solutions of 1 mM MV^{2+} in 0·10 M SDS and quickly annealed to room temperature. The resonance field position for DPPH is represented by the vertical arrow. (From Colaneri *et al.* (1987).)

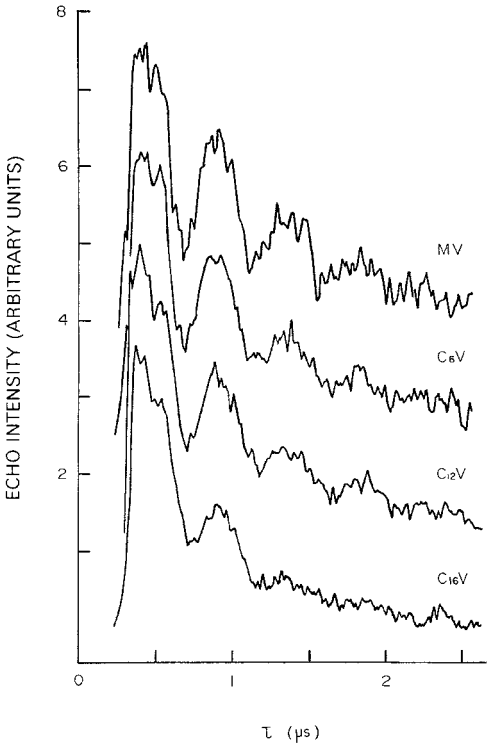

Figure 5. Two-pulse ESE decay spectra at the X band obtained from 77 K ultraviolet-irradiated alkylmethylviologens in DHP vesicles prepared in D_2O. The ESE spectra were recorded at 4·2 K. The baselines are offset vertically for spectral comparisons. (From Colaneri *et al.* (1987).)

splitting and the g factor identify the species as the methylviologen monocation (Colaneri *et al.* 1987). Alkylmethylviologens give similar spectra.

Figure 5 shows the two-pulse echo intensity against interpulse time for photoreduced methylviologen and several alkylmethylviologens in frozen solutions of dihexadecylphosphate (DHP) vesicles prepared in deuterated water. The modulation is very prominent and the period indicates that it is associated with interactions from deuterium, and hence from deuterated water at the vesicle interface. Some protium modulation is also observed which has a period 6·6 times smaller than that of deuterium. It is seen that the deuterium modulation depth gets weaker as the alkyl chain length increases. Thus there seems to be a significant alkyl chain length effect on the location on the alkylmethylviologen relative to the interface in the DHP vesicles. Figure 6 shows similar results in frozen SDS micellar systems prepared in deuterated water. Here again deuterium modulation is detectable but it is not as prominent as it was in the vesicle system. Also the effect of the alkyl chain length on the deuterium modulation depth is relatively weak and must be analysed quantitatively to detect a trend, if any. Figure 7 shows a plot of normalized modulation depth against alkylmethylviologen chain length derived from the data in figures 5 and 6. As seen qualitatively from those figures, figure 7 shows a strong and definite alkyl chain length effect for photoreduction in DHP vesicles and a much weaker alkyl chain length effect, if any, in SDS micelles. In addition to this difference, the magnitude of the normalized modulation depth is very different in the vesicle and in the micelle systems. The lower magnitude in the micelle system indicates that the viologen moiety is less exposed to water at the interface than in the vesicle system (Colaneri *et al.* 1987).

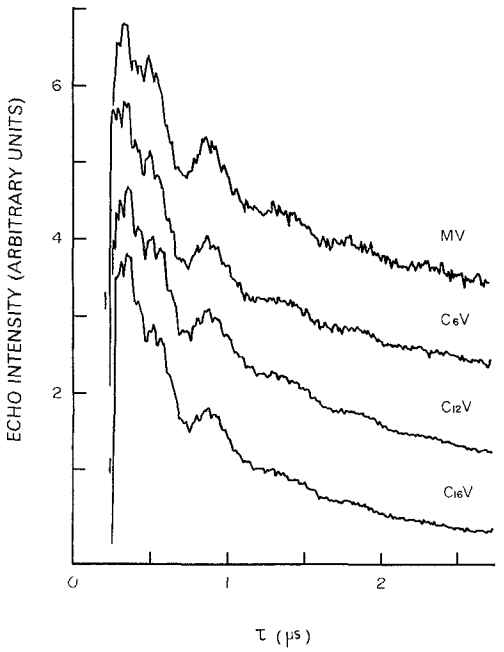

Figure 6. Two-pulse ESE decay spectra at the X band obtained from 77 K ultraviolet-irradiated alkylmethylviologens in SDS micelles prepared in D_2O. The ESE spectra were recorded at 4·2 K. The baselines are vertically offset for spectral comparisons. (From Colaneri *et al.* (1987).)

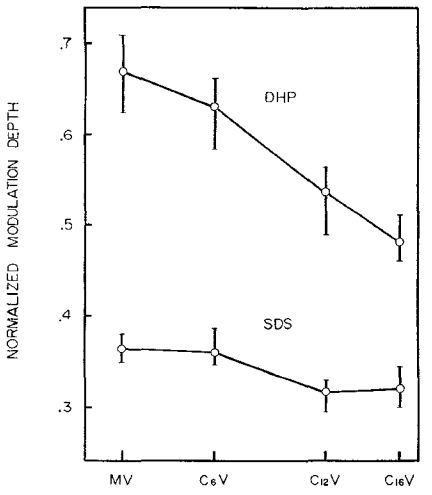

Figure 7. Plots showing the dependence of the measured ESE normalized modulation depths at $\tau \approx 0{\cdot}75$ μs on the alkyl chain length of the alkylmethylviologen radical monocations in SDS micelles and DHP vesicles. The upper curve gives this dependence in the vesicle system, and the lower curve is the micelle system. The spread of measured values is depicted by the vertical bars. (From Colaneri *et al.* (1987).)

The data in figure 7 can be interpreted in terms of the schematic structural model for the alkylmethylviologens with respect to the surfactant assembly interfaces as shown in figure 8. The interface of a SDS micelle has a relatively high surface roughness indicated by some dispersion in the locations of the head-groups of the surfactant molecules at the surface of the micelle. This allows the alkylmethylviologen to penetrate relatively deeply into the interface region even for short alkyl chains and there is little difference in the depth of penetration as a function of alkyl chain length. However, there appears to be some. Furthermore, since the alkylmethylviologen is embedded relatively deeply into the interface the interaction with water is relatively weak as indicated by the lower value of the normalized deuterium modulation depth. However, in the DHP vesicle system the interface is more ordered with a low surface roughness and the bilayer structure formed by the alkyl chains of the surfactant molecule is also more ordered. Both factors make it more difficult for the alkylmethylviologen to penetrate into the vesicle. So for a short alkyl chain length such as dimethylviologen the viologen moiety is relatively more exposed to water at the vesicle interface and interacts much more strongly than it does in the micellar system. Also the longer alkyl chain has a definite and significant effect on the interplay of the hydrophobic interactions and causes the viologen moiety to penetrate more deeply into the interface region. This is particularly exciting because it illustrates that location control of the photoreducible part of an electron acceptor can be achieved by varying the length of the alkyl chain over reasonable lengths (Colaneri *et al.* 1987). In later work it is shown that this location control of alkylmethylviologens relative to the interface of the surfactant does in fact correlate with the photoreduction yield. The control of alkylmethylviologens also correlates with electron acceptor kinetics studied in the liquid phase by optical means (Thompson *et al.* 1987). This further supports the assertion that the structural results in frozen solutions are related to the same structural factors that are applicable to liquid phase systems.

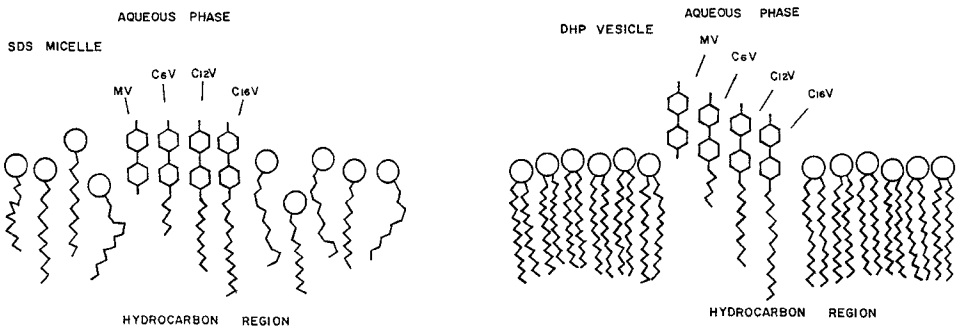

Figure 8. A schematic diagram illustrating the relative locations of the various alkylmethylviologen radical monocations in the interface regions of the SDS micelles (left-hand side) and the DHP vesicles (right-hand side). (From Colaneri *et al.* (1987).)

A more ambitious experiment is to try to control the location of both an electron donor and a specific electron acceptor within a micelle or vesicle. This has been done for alkylated ruthenium *tris*(bipyridyl) species as electron donors and alkylmethylviologens as electron acceptors in SDS micellar systems (Colaneri *et al.* 1989). Figure 9 shows a schematic diagram of this experiment where the ruthenium *tris*(bipyridyl) species penetrate the SDS micellar interface significantly if an alkyl chain is added to one of the pyridine rings. It then penetrates the interface to a significant extent. Figure 10 demonstrates that specific electron transfer does occur from the ruthenium *tris*(bipyridyl) species to the alkylmethylviologen by photoirradiation at 430 nm in the ruthenium *tris*(bipyridyl) band in a frozen micellar solution at 77 K. If only the ruthenium *tris*(bipyridyl) is present, no net ESR signal is seen and, if only the methylviologen is present, no ESR signal is seen. In the latter case that is because methylviologen does not absorb the 430 nm light which the ruthenium *tris*(bipyridyl) species does. However, in figure 10 (*b*) if both the ruthenium *tris*(bipyridyl) species and the methylviologen acceptor are present, a stable ESR spectrum is generated which is identified as the methylviologen cation from its g factor or by resolved hyperfine structure upon warming the micellar solution to the liquid phase. Thus the methylviologen cation that is observed must be formed by electron transfer from a photoexcited ruthenium *tris*(bipyridyl) species.

Figure 11 shows a plot of a comprehensive series of experiments where four different alkylated ruthenium *tris*(bipyridyl) molecules were photoexcited in the presence of a series of alkylmethylviologens of varying alkyl chain lengths from C_1 to C_{20}. In this case the ESR intensity represents the intensity of the photoreduced alkylmethylviologen cation which reflects the efficiency of net photo-ionization in the system. If we first look at the results for the ruthenium *tris*(bipyridyl) species itself, it is seen that the photoyield decreases slowly as the alkylmethylviologen chain length increases. This is consistent with the direct photoreduction results shown in figure 7 where the deuterium modulation depth was plotted against the alkylmethylviologen chain length. Again, the effect in micellar systems is relatively weak but, to the extent of the alkyl chain lengths investigated, it is clear that in the micellar systems there is a small but significant alkyl chain length effect in the direction expected.

The particularly interesting aspect of figure 11 is that, if an alkyl chain is added to a bipyridine ring of the ruthenium *tris*(bipyridyl) species, there is a significant effect on the photo-ionization yield for a specific range of alkylmethylviologen chain lengths. This

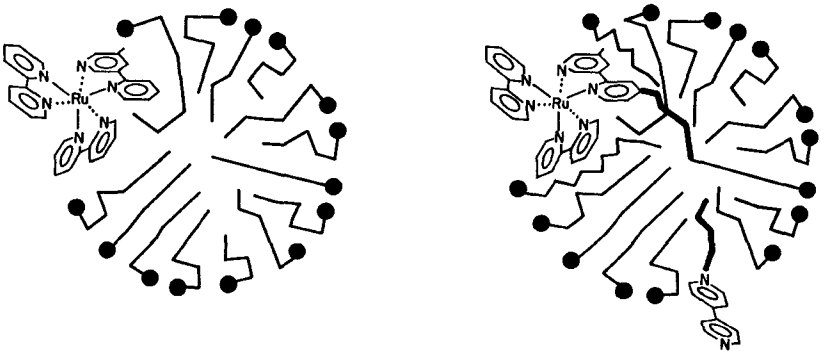

(a) (b)

Figure 9. Schematic diagrams of (*a*) $Ru(bpy)_3^{2+}$ in SDS micelles and (*b*) alkylated $Ru(bpy)_3^{2+}$ [$Ru(bpy)_2(bpy\text{-}C_n)^{2+}$] with $C_n \equiv C_5$, C_{13} or C_{17} and alkylmethylviologen (C_nV^{2+}) with $n \simeq 6$ in SDS micelles.

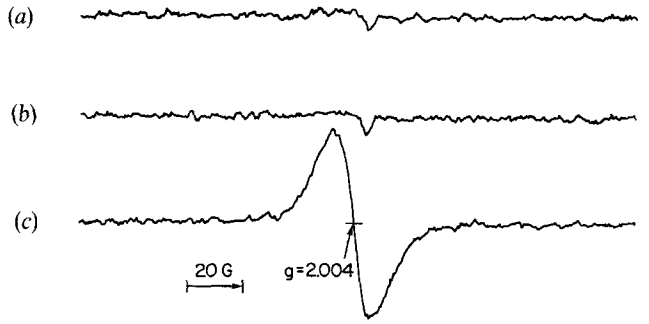

Figure 10. X-band ESR spectra at 77 K recorded from ultraviolet-irradiated frozen 0·05 M SDS solutions containing (*a*) 0·5 mM $Ru(bpy)_3^{2+}$, (*b*) 2·5 mM MV^{2+} and (*c*) 0·5 mM $Ru(bpy)_3^{2+}$ and 2·5 mM MV^{2+}. (From Colaneri *et al.* (1989).)

must mean that an alkyl chain attached to a bipyridyl ring of a ruthenium *tris*(bipyridyl) species has a specific localization effect with respect to the micellar interface which enhances the probability of electron transfer. Since there is no significant difference between the results for C_5, C_{13} or C_{17} alkyl chains on the ruthenium *tris*(bipyridyl) species it suggests that this species is too bulky to be pulled into the interface very much by an alkyl chain and that a longer alkyl chain does not change the location appreciably. Moreover, it is significant that an alkyl chain of only five carbons has the power to localize an alkylated ruthenium *tris*(bipyridyl) species so that it is in a more favourable position at the micellar interface for photoinduced electron transfer. The fact that the photo-ionization efficiency is most enhanced for an alkylmethylviologen chain length of C_6 to C_8 implies the existence of a sort of 'resonance' effect on the photo-ionization yield. It was shown in the previous experiments, as illustrated in figures 7 and 8, that the alkyl chain length on an alkylmethylviologen does tune the position of the viologen moiety with respect to the surfactant assembly interface. In the experiment shown in figure 11 the ruthenium *tris*(bipyridyl) is fixed in a particular position at the interface, and tuning of the electron acceptor position relative to the interface is expected to be optimum for electron

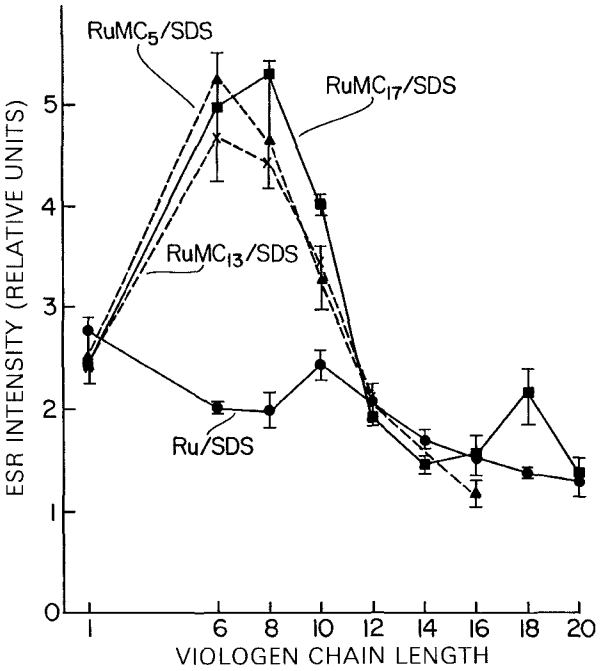

Figure 11. ESR signal intensity dependences on alkylmethylviologen chain length for ultraviolet-irradiated frozen 0·05 M SDS solutions containing either 0·5 mM $Ru(bpy)_3^{2+}$, $Ru(bpy)_2(bpy\text{-}C_5)^{2+}$, $Ru(bpy)_2(bpy\text{-}C_{13})^{2+}$ or $Ru(bpy)_2(bpy\text{-}C_{17})^{2+}$ and 2·5 mM viologen. Alkylmethylviologen alkyl chain lengths are 1 (methylviologen), 6, 8, 10, 12, 14, 16, 18 and 20. (From Colaneri *et al.* (1989).)

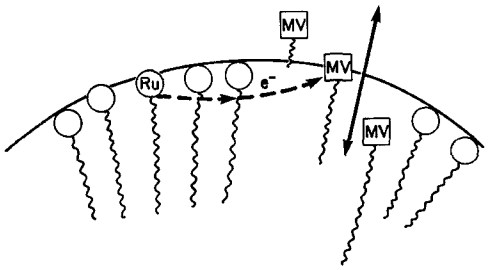

Figure 12. Schematic diagram of electron transfer geometry from alkylated $Ru(bpy)_3^{2+}$ species (Ru-alkyl) to alkylmethylviologen (MV-alkyl) in SDS micelles (O-alkyl). The vertical arrow indicates that the position of the viologen moiety of the alkylmethylviologen can be tuned relative to the micelle interface or surface by the length of the alkyl chain.

transfer for a particular alkyl chain length. This is indeed what is observed and it is rather exciting that this can be achieved and demonstrated. Figure 12 shows a schematic diagram of this interpretation.

5. Radical conversion

A photoinduced radical conversion process in the photoreduction of alkylmethylviologens in frozen vesicle systems has been discovered which enables the net photo-ionization efficiency to be increased (Sakaguchi and Kevan 1989). The

radical conversion is from the photoreduced alkylmethylviologen radical to a surfactant radical localized on an alkyl chain of the surfactant. The advantage of this photoinduced radical conversion is that it provides an additional barrier to back electron transfer and hence increases the net photo-ionization yield. The efficiency of this effect is significantly dependent upon the surface charge of the vesicle system. Figure 13 shows ESR spectra for the photoreduction yield of alkylmethylviologens of varying alkyl chain length in dioctadecyldimethylammonium chloride (DODAC) vesicles which have a positive interface charge. In addition to the strong line due to the alkylmethylviologen radical cation, weak lines are seen which become more prominent the longer the alkyl chain and which have been found to be associated with a surfactant radical. These ESR lines associated with surfactant radicals are weak in dipalmitoylphosphatidylcholine (DPPC) vesicles with a nominally neutral interface and are not seen in dihexadecylphosphate (DHP) vesicles with a negatively charged interface. Thus this process was not detected in earlier work in which only DHP vesicles were studied as was shown above in figure 5 (Colaneri *et al.* 1987).

Figure 14 shows how the surfactant radical was identified. At longer photolysis times the surfactant radical lines become more prominent and eventually only the surfactant radical is present in the ESR spectrum. In figure 14(*c*) the ESR spectrum is analysed to give an octet splitting of 2·2 mT with relative intensities consistent with a

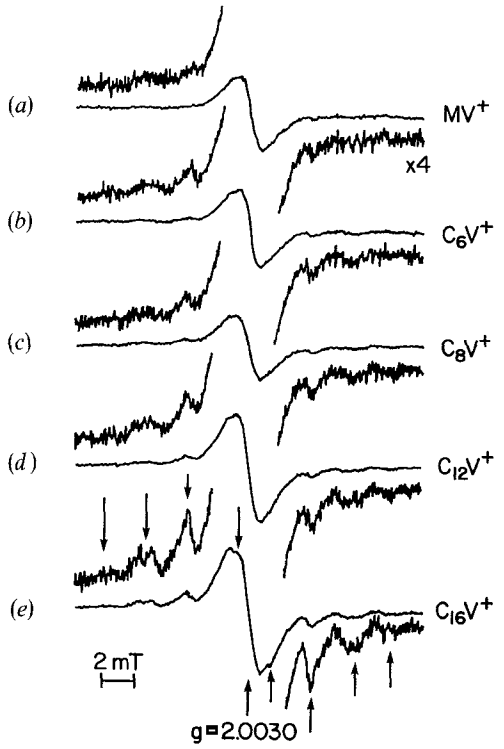

Figure 13. ESR spectra at 77 K from alkylmethylviologens in DODAC vesicles after 10 min photoirradiation: (*a*) MV^+; (*b*) C_6V^+; (*c*) C_8V^+; (*d*) $C_{12}V^+$; (*e*) $C_{16}V^+$. The outer parts of the singlet spectra are shown with a four times higher gain. (From Sakaguchi and Kevan (1989).)

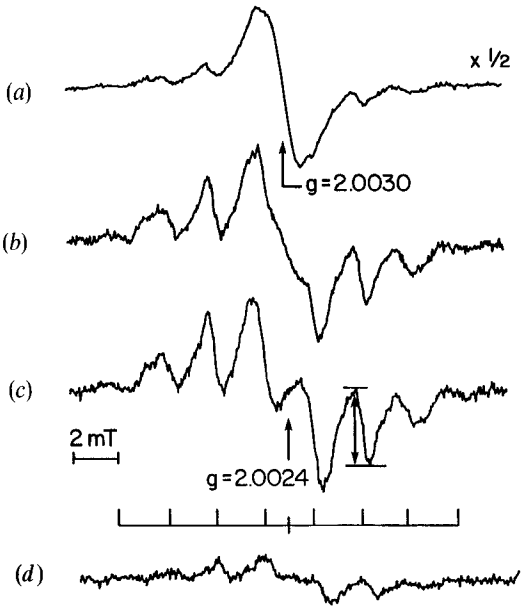

Figure 14. ESR spectra from $C_{16}V^+$ in DODAC vesicles after photoirradiation for (*a*) 10 min, (*b*) 72 min and (*c*) 200 min and (*d*) the background spectrum from DODAC vesicles without C_nV^{2+} irradiation for 200 min. The stick diagram in (*c*) indicates the hyperfine pattern of the octet spectrum. (From Sakaguchi and Kevan (1989).)

secondary alkyl radical. Thus the surfactant radical in this system is identified as the DAC radical, a secondary radical on one of the alkyl chains, of a DODAC molecule.

Figure 15 shows that this photoinduced radical conversion occurs with no change in the total spin concentration. It is seen that with increasing photolysis time the intensity of the alkylmethylviologen radical decreases in a correlated fashion with the increase in the DAC surfactant radical. It has been suggested that the photoinduced radical conversion occurs by H abstraction from some position on a surfactant alkyl chain followed by H migration along the alkyl chain to end up with a secondary radical. This interpretation is supported by figure 16 which shows the radical yield plotted against the alkyl chain length of the alkylmethylviologen. As was indicated in the ESR spectra, the radical yield increases with increasing alkyl chain length in both the DODAC and the DPPC vesicle systems. This is consistent with greater interface insertion for the longer-chain alkylmethylviologens which gives a greater probability of radical conversion to the surfactant alkyl chain.

Once the hydrogen abstraction process has taken place, the occurrence of hydrogen migration along the surfactant alkyl chain is directly supported by the ESEM results shown in figure 17. Note that the normalized deuterium modulation for the DAC radical is significantly lower than that for the alkylmethylviologen radical in the DODAC vesicle system. This implies that the DAC radical location is inserted much more deeply into the vesicle than is the viologen moiety of the alkylmethylviologen radical cation. This is consistent with a secondary alkyl radical location for the surfactant radical.

It is also interesting to note from figure 17 that the deuterium modulation depth is less for alkylmethylviologen cation radicals in cationic DODAC vesicles than in

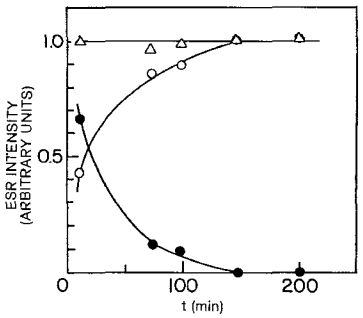

Figure 15. Relative ESR intensity at 77 K against irradiation time τ for $C_{16}V^+$ in DODAC vesicles: (△), total ESR intensity; (○), octet spectrum from DAC; (●), singlet spectrum from $C_{16}V^+$. (From Sakaguchi and Kevan (1989).)

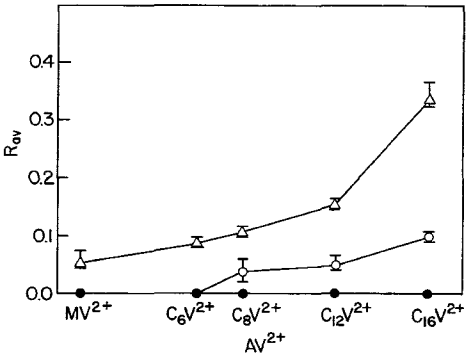

Figure 16. Relative ESR intensities R_{av} after 10 min irradiation at 77 K of the octet surfactant radical against the alkyl chain length of C_nV^{2+} in DODAC (△), DPPC (○) and DHP (●) vesicles. (From Sakaguchi and Kevan (1989).)

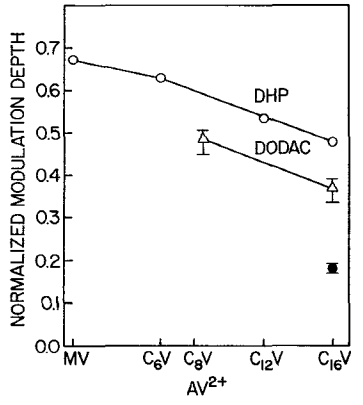

Figure 17. Normalized deuterium modulation depth against alkyl chain length in C_nV^{2+}: (△), C_nV^+ in DODAC vesicle irradiated for 10 min; (●) DAC from $C_{16}V^+$ in DODAC vesicle irradiated for 200 min. (From Sakaguchi and Kevan (1989).)

anionic DHP vesicles. This indicates that the alkylmethylviologen radical cation penetrates deeper into the vesicle interface in the cationic vesicle system. If this penetration is deep enough, repulsion from the cationic interface may occur. Thus both alkyl chain length effect and the charge effect are important for viologen binding at these vesicle interfaces.

Finally figure 18 shows the net photo-ionization yields in the DODAC, DPPC and DHP vesicle systems as a function of the alkylmethylviologen. It is seen that there is both an alkyl chain length effect and an interface charge effect in the net photo-ionization yield such that optimal charge separation occurs for the longest alkyl chains on the alkylmethylviologen electron acceptor and for a positively charged interface. This is due to the radical conversion process as well as to the probability for electron escape across the charged vesicle interface.

6. Photo-ionization of alkylphenothiazine sulphonates in vesicles and micelles

A series of alkylphenothiazine sulphonates has been used to test location control via variable-length alkyl chains on the photo-ionization of a donor in vesicles (Sakaguchi *et al.* 1990), micelles (Baglioni *et al.* 1990) and reverse micelles (Hu and Kevan 1990). Figure 19 shows the structures of two different types of alkylphenothiazine sulphonate. In the PC_nS series the alkyl chain is attached to the phenothiazine with variable-length alkyl chains terminated in a sulphonate group. The polar sulphonate group is expected to localize in the interface region of a surfactant assembly with the phenothiazine moiety located to different depths in the surfactant assemblies depending upon the alkyl chain length. The C_nPS series has the sulphonate group attached to the phenothiazine aromatic ring and localizes this entity at the interface of a surfactant assembly with an alkyl chain of variable length extending into the non-polar region of the assembly.

Figure 20 shows the photo-ionization yield for these two types of alkylphenothiazine sulphonates as a function of alkyl chain length in cationic DODAC vesicles and anionic DHP vesicles. In the cationic DODAC vesicles there is an alkyl chain length effect in the direction such that the photo-ionization yield is less for a longer alkyl chain. In the PC_nS series it appears that the phenothiazine moiety is pushed deeper into the vesicle away from the interface by a longer alkyl chain. This is the behaviour expected of the most simple model in which the alkyl chain does not show a significant degree of bending in the vesicle interior. This interpretation is fully

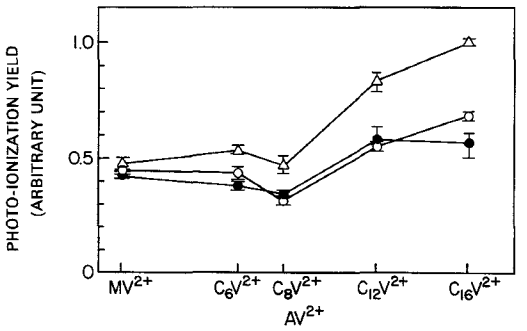

Figure 18. Photoirradiation yield at 77 K from C_nV^{2+} in vesicles for 10 min irradiation against alkyl chain length in C_nV^{+}: (△), DODAC; (○), DPPC; (●), DHP. (From Sakaguchi and Kevan (1989).)

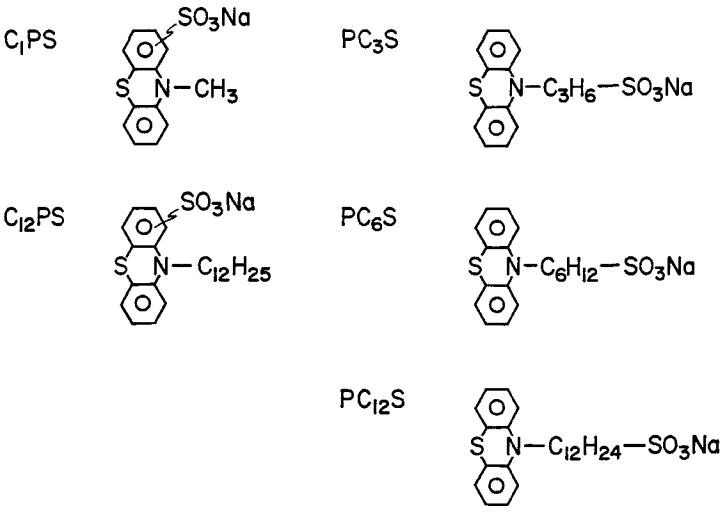

Figure 19. Structures and abbreviations of the alkylphenothiazine sulphonates studied.

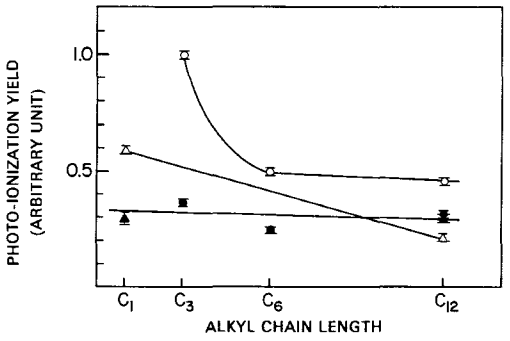

Figure 20. Photoirradiation yield at 77 K from alkylphenothiazines in vesicles for 10 min irradiation with $\lambda > 300$ nm against the alkyl chain length: (○), PC_nS ($n=3,6,12$) in DODAC vesicles; (△), C_nPS ($n=1,2$) in DODAC vesicles; (●), PC_nS ($n=3$, 6, 12) in DODAC vesicles; (△), C_nPS ($n=1,2$) in DODAC vesicles; (●), PC_nS in DHP vesicles; (▲), C_nPS in DHP vesicles. (From Sakaguchi *et al.* (1990).)

supported by the ESE deuterium modulation results for the PC_nS systems shown in figure 21.

For the C_nPS series of molecules the photo-ionization yield is less than for the PC_nS series of molecules and the phenothiazine moiety is expected to be at the interface. The low yield is therefore perhaps due to a more efficient back electron transfer for this interface location. The alkyl chain length effect that is observed indicates that the C_{12} chain does have some influence on burying the phenothiazine moiety deeper into the interface so that the photoelectron transfer is inhibited somewhat and the net photo-ionization yield decreases. This again is supported by the ESE deuterium modulation depth results shown in figure 21.

In the anionic DHP vesicles the results are rather different in that no effect of the alkyl chain length is seen for either the PC_nS or the C_nPS series of molecules (figure 20).

However, for the PC_nS series of molecules the ESE deuterium modulation depth results (figure 21) show that the alkyl chain length effect on the location occurs in the same way that it does in the cationic DODAC vesicles. The insensitivity of the photo-ionization yields to this difference in location control by the alkyl chain length is thus probably related to the opposite interface charge.

For the C_nPS series of molecules in anionic DHP vesicles the relatively large ESE deuterium modulation depths shown in figure 21 support the fact that there is little embedment of this type of molecule into the vesicle interface. This, in turn, is consistent with the relatively low photo-ionization yields given in figure 20. It is also true that less embedment of this series of molecules into the interface is consistent with less photoinduced radical conversion as observed.

The photoyield results for the PC_nS series of molecules in sodium alkylsulphate anionic micelles are shown in figure 22. These results contrast significantly with the trends seen in anionic vesicles for this same series of photo-ionizable molecules. The photoyields increase with increasing alkyl chain lengths in the PC_nS series of molecules and perhaps reach a maximum for PC_6S. This maximum photoyield and an intermediate alkyl chain length are consistent with more alkyl chain bending which could be a reflection of the greater internal disorder in micelles compared with vesicles. This trend in the photoyields is fully supported by trends in the normalized deuterium modulation depths as shown in figure 23. A similar trend in photoyields is found in cationic alkyltrimethylammonium bromine micelles.

Also shown in figures 22 and 23 is an effect of the alkyl chain length *of the surfactant* on the photoyields and deuterium modulation depths. The photoyields are largest for the shorter C_{10} alkyl chain in the surfactant and the shorter alkyl chain surfactant also shows the greatest deuterium modulation depth which is consistent with this. It is noted that the correlation of the deuterium modulation depth with the photoyields is consistent with embedded photo-ionizable PC_nS molecules.

However, the C_nPS series of molecules show quite different results as illustrated in figure 24. There the photoyield anticorrelates with the deuterium modulation depth. The anticorrelation seems consistent with C_nPS not being embedded very deeply into the anionic micellar interface.

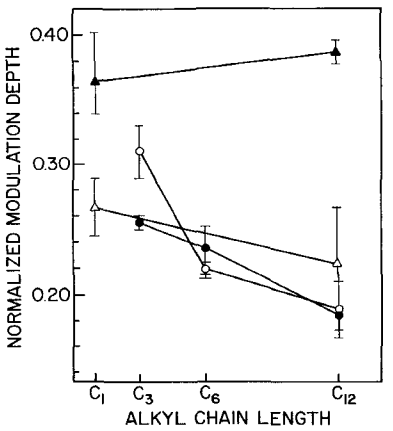

Figure 21. Normalized deuterium modulation depth from alkylphenothiazines in vesicles for 10 min irradiation with $\lambda > 300$ nm against the alkyl chain length: (○), PC_nS ($n = 3, 6, 12$) in DODAC vesicles; (△), C_nPS ($n = 1, 2$) in DODAC vesicles; (●), PC_nS in DHP vesicles; (▲), C_nPS in DHP vesicles. (From Sakaguchi *et al.* (1990).)

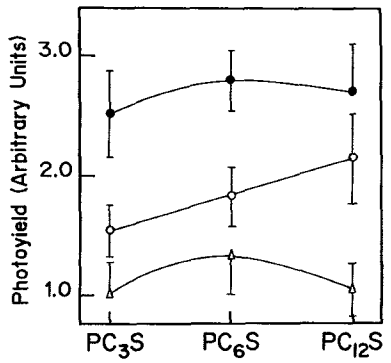

Figure 22. PC_nS photocation yield measured by ESR as a function of PC_nS alkyl chain length in micellar solutions of sodium alkylsulphate surfactants: (●), $n=10$; (△), $n=12$; (○), $n=14$. (From Baglioni *et al.* (1990).)

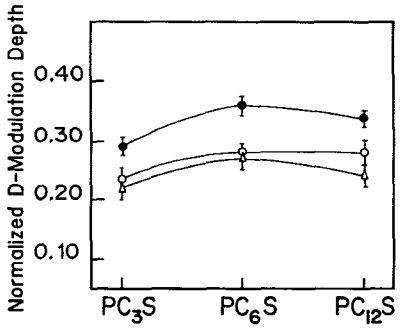

Figure 23. Normalized deuterium modulation depth as a function of PC_nS alkyl chain length in micellar solutions of sodium alkylsulphate surfactants: (●), $n=10$; (△), $n=12$; (○), $n=14$. (From Baglioni *et al.* (1990).)

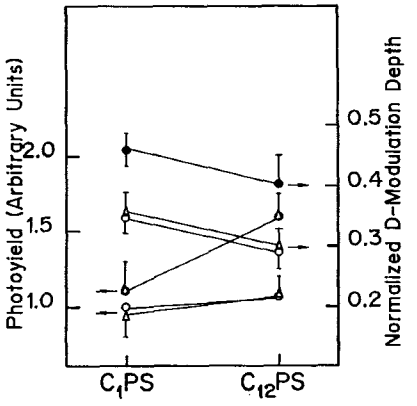

Figure 24. Normalized deuterium modulation depth and photocation yield, measured by ESR, as a function of C_nPS alkyl chain length in micellar solutions of sodium alkylsulphate surfactants: (●), $n=10$; (△), $n=12$; (○), $n=14$. (From Baglioni *et al.* (1990).)

Similar trends are observed for C_nPS molecules in catonic alkyltrimethylammonium bromide micelles where it is also concluded that the C_nPS molecules are not embedded very deeply into the cationic micelle interface. Thus the micellar surface charge does not seem to influence the C_nPS molecule locations very much. To make the

picture clearer, a schematic diagram of the location control of the PC_nS and the C_nPS series of photo-ionizable molecules is shown in figure 25. The PC_nS series is shown in figure 25 (*a*). A lower yield is implied for the C_3 chain which is too short to bend and forces the phenothiazine moiety to be relatively deeply embedded into the micellar interior. However, for the C_6 alkyl chain, significant bending can occur to locate the phenothiazine moiety relatively near the interface with a corresponding increase in the photo-ionization yield. Similar bending occurs for the C_{12} alkyl chain except that the greater chain length allows the phenothiazine moiety to probe a greater volume and hence it penetrates less into the interface than it does for a C_6 alkyl chain. This interpretation is consistent with the experimental photoyield results. A similar schematic model is applicable to vesicles except that there is less alkyl chain bending owing to the more ordered vesicle interior so that the photo-ionization yields are constant with alkyl chain length (anionic DHP vesicles) or decrease slowly with increasing alkyl chain length (cationic DODAC vesicles).

In figure 25 (*b*) a schematic diagram is shown of the C_nPS molecular positions relative to the interface. For both short and long chains the phenothiazine moiety is very near the interface but for a longer alkyl chain the hydrophobic effect of the chain plays a role and draws the charged phenothiazine moiety a little deeper into the interface, which is consistent with an increased photoyield in this case due to less back electron transfer. A similar schematic model is applicable to anionic vesicles.

7. Photo-ionization of alkylphenothiazine sulphonates in reverse micelles

The same PC_nS and C_nPS series of molecules were investigated in two different reverse micellar systems (Hu and Kevan 1990). One is the well known AOT surfactant which is sodium *bis*(2-ethyl-1-hexyl)sulphosuccinate which forms reverse micelles in a non-polar solvent such as iso-octane. It should be noted that the alkyl chain is branched in the AOT surfactant. The other reverse micellar system is formed from cetyltrimethylammonium bromide (CTAB) surfactant together with a short-chain alcohol as co-surfactant. The co-surfactant is necessary to lower the interfacial tension between water and the organic phase in order to form reverse micelles. It is possible to modify this CTAB reverse micellar system with respect to interface polarity by changing the co-surfactant from 1-butanol to 1-hexanol to 1-octanol. Figure 26 shows relative photo-ionization yields in these reverse micellar systems as a function of the alkyl chain length in the PC_nS series of molecules.

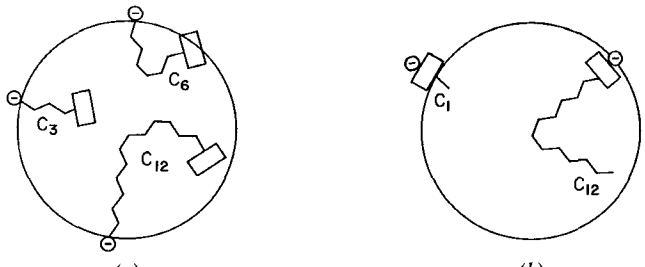

Figure 25. Schematic diagrams of location of phenothiazine derivatives in ionic micelles (*a*) PC_nS molecules and (*b*) C_nPS molecules where the circle represents the sulphonate group and the rectangle represents the phenothiazine moiety. (From Baglioni *et al.* (1990).)

Photoinduced conversion of the cation radicals of phenothiazine and methylviologen to surfactant alkyl radicals occurs in vesicles at 77 K (Sakaguchi and Kevan 1989, Sakaguchi *et al.* 1989). A similar photoinduced conversion occurs in CTAB reverse micelles with 1-butanol as co-surfactant. This conversion is prevented by a decrease in the polarity of the reverse micelle by changing the co-surfactant to 1-hexanol or 1-octanol. The cation radical interacts more strongly with the more polar co-surfactant, and photoinduced conversion to an alkyl radical, probably from the co-surfactant, occurs more easily. The results suggests that photoinduced conversion to a surfactant alkyl radical is inhibited in a reverse micelle without a polar co-surfactant. AOT reverse micelles have no co-surfactant and show mainly a singlet signal characteristic of the cation radical of phenothiazine.

The probable locations of the photo-ionizable molecules in the reverse micelles are as follows. All the components of CTAB reverse micelles have straight alkyl chains which pack more compactly than branched alkyl chains. Figure 27(*a*) shows a schematic structure of CTAB micelles with embedded photo-ionizable molecules. PC_3S has a charged sulphonate group at the end of a three-carbon aliphatic chain; so this charged end is expected to be at the polar interface of the micelle. The other end of

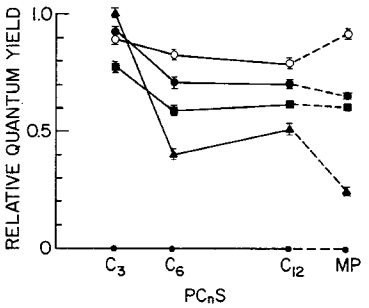

Figure 26. Relative photo-ionization yield against the alkyl chain length of alkyl phenothiazines (PC_3S, PC_6S and $PC_{12}S$) and comparison with the relative photo-ionization yields of methylphenothiazine (MP) for 1-butanol (■), 1-hexanol (●) and 1-octanol (▲) in CTAB reverse micelles and in AOT micelles (○). (From Hu and Kevan (1990).)

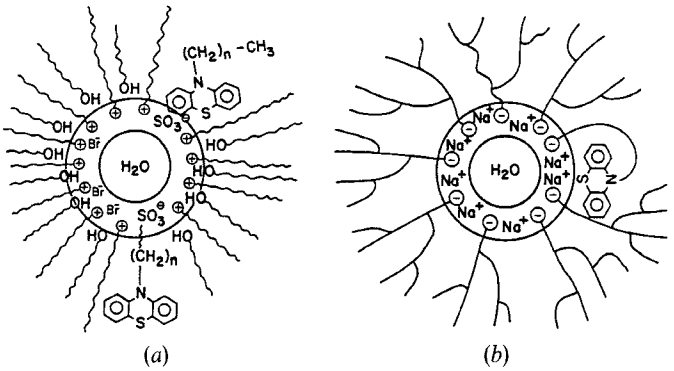

Figure 27. (*a*) Schematic structure of CTAB reverse micelles with embedded photo-ionizable molecules: (⊕~~~~), CTAB; (HO~~~~), co-surfactant. (*b*) Schematic structure of AOT reverse micelles where the branched structure represents AOT. (From Hu and Kevan (1990).)

the molecule with the phenothiazine chromophore is expected to extend into the organic bulk phase. The chromophores of the similar molecules, PC_6S and $PC_{12}S$, are probably located farther from the interface into the organic bulk phase because they have longer alkyl chains. Compounds C_1PS and $C_{12}PS$ have the charged sulphonate group on the chromophore. This charged group should locate the chromophore in the interface. $C_{12}PS$ has a longer aliphatic chain which could 'pull' the chromophore towards the non-polar organic phase to a greater extent than for C_1PS. Methylphenothiazine (MP) is a less polar molecule without a charged group. It is expected to extend more into the non-polar organic phase than C_nPS molecules but less so than PC_nS molecules.

The different location of the chromophores in CTAB reverse micelles is interpreted as the major cause of the differences in the photo-ionization yields. In figure 26 it is seen that PC_3S has the highest photo-ionization yield in CTAB reverse micelles for different co-surfactants. The yield is higher than for those molecules with chromophores farther away from the interface, such as PC_6S, $PC_{12}S$ and MP. However, the yield for $PC_{12}S$ is not lower than that for PC_6S, indicating some chain bending for $PC_{12}S$. The yield for PC_3S is also higher than for those molecules with chromophores in the interface, such as C_1PS and $C_{12}PS$. This suggests that back electron transfer reduces the yields for C_1PS and $C_{12}PS$ since they are more exposed to the water phase. Also the sulphonate group, which has a slight electron withdrawal effect on the chromophore, may cause a decrease in the yield. It appears that PC_3S locates the chromophore in a more optimal position for photo-ionization than do the other molecules studied.

Comparing the molecules C_1PS and $C_{12}PS$, it is seen that $C_{12}PS$ has the higher photo-ionization yield. This result is consistent with the results found for alkylmethylviologen in micelles and vesicles (Colaneri *et al.* 1987, Sakaguchi and Kevan 1989). This is explained by a shift of the chromophore towards the organic phase which is caused by the long alkyl tail in $C_{12}PS$. However, note that this effect is smaller than the effect between PC_3S and PC_6S.

It is also of interest to compare the photo-ionization yields of MP and C_1PS in which the difference is the sulphonization of the phenothiazine moiety. In general it is expected than the C_1PS yield will be higher since it is expected to be closer to the water phase. This is the case for the CTAB/C_8OH reverse micelle, but this is not the case for the CTAB/C_6OH, CTAB/C_4OH or AOT systems. In these cases it is suggested that the C_1PS yield is anomalously low due to back electron transfer. In fact, the MP yield in CTAB/C_8OH seems anomalously low and suggests that MP is particularly well solubilized into the organic phase in CTAB/C_8OH.

Figure 26 also shows that the photo-ionization yield with 1-octanol as co-surfactant is highest for PC_3S but lowest for PC_6S, $PC_{12}S$ or MP compared with 1-hexanol or 1-butanol co-surfactants. This might be explained by less alkyl chain bending of the less polar surfactant. Thus the photo-ionization yields seem sensitive to alkyl-chain-enforced location of the chromophore as well as to modification of this location by the surfactant polarity.

AOT is a surfactant with a branched alkyl chain. Figure 27(*b*) shows a schematic structure of AOT micelles. AOT micelles also contain a branched organic solvent (iso-octane) in the bulk phase. These branched chains seem to allow more alkyl chain bending for the straight-chain photo-ionizable molecules (PC_3S, PC_6S and $PC_{12}S$) to locate the chromophore nearer to the interface. This is reflected by the similar photo-ionization yields of PC_3S, PC_6S and $PC_{12}S$ in AOT reverse micelles. The high photo-ionization yield for MP in AOT reverse micelles suggests that MP is located

more into the interface than are the PC_nS molecules which is consistent with the lower polarity of MP.

8. Conclusions

The results summarized in this review show clearly that location control of photo-ionizable donors and acceptors relative to the interfaces of surfactant assemblies such as micelles and vesicles is practical by use of variable-length alkyl chains on the donors and acceptors. It also appears that the degree of control is generally greater in vesicles than in micelles. This appears to be related to the greater degree of interior order in vesicles than in micelles so as to inhibit alkyl chain bending to some extent. ESEM is particularly effective for monitoring the degree of location control and serves as a very sensitive probe of this structural variation.

In addition to variable-length alkyl chains as a primary control factor, several secondary control factors have also been identified which may be used to advantage in some cases and may be a complication in others. One secondary control factor includes the interface charge and the donor charge. This can affect the degree of embedment into the interface and controls whether back electron transfer is important or not. A second control factor is the size of the donor or acceptor. If either one is too large, as ruthenium *tris*(bipyridyl) appears to be, little penetration into the interface will occur for steric reasons and the yield is correspondingly lower than expected owing at least partially to back electron transfer. A third control factor is the occurrence of photoinduced radical conversion from the radical cation to a surfactant radical. In general such photoinduced radical conversion is favourable for increasing the net photo-ionization yield owing to a greater barrier to back electron transfer. A fourth control factor is the degree of alkyl chain bending which depends on the interior order of the surfactant assembly and also on whether the surfactant assembly alkyl chains are branched or not.

Acknowledgment

This research was supported by the Division of Chemical Sciences, Office of Basic Energy Sciences, Office of Energy Research, U.S.A. Department of Energy.

References

BACHMAN, L., DASCH, W., and KUTTER, P., 1981, *Ber. Bunsenges. phys. Chem.*, **85,** 883.
BAGLIONI, P., HU, M., and KEVAN, L., 1990, *J. phys. Chem.*, **94,** 2586.
BAGLIONI, P., and KEVAN, L., 1987, *J. phys. Chem.*, **91,** 1516.
COLANERI, M. J., KEVAN, L., and SCHMEHL, R., 1989, *J. phys. Chem.*, **93,** 397.
COLANERI, M. J., KEVAN, L., THOMPSON, D. H. P., and HURST, J. K., 1987, *J. phys. Chem.*, **91,** 4072.
GRÄTZEL, M., 1988, *Heterogeneous Photochemical Electron Transfer* (Boca Raton, Florida: CRC).
HASHIMOTO, S., and THOMAS, J. K., 1983, *J. Am. chem. Soc.*, **105,** 5230.
HIROMITSU, I., and KEVAN, L., 1986, *J. phys. Chem.*, **90,** 3088.
HU, M., and KEVAN, L., 1990, *J. phys. Chem.*, **94** (to be published).
KEVAN, L., 1979, *J. phys. Chem.*, **70,** 6006; 1981, *Ibid.*, **85,** 1628; 1988, *Photoinduced Electron Transfer* Part B: *Experimental Techniques and Medium Effects*, edited by M. A. Fox and M. Channon (Amsterdam: Elsevier), p. 329.
LI, A. S. W., and KEVAN, L., 1983, *J. Am. chem. Soc.*, **105,** 5752.
NARAYANA, P. A., LI, A. S. W., and KEVAN, L., 1981, *J. Am. chem. Soc.*, **103,** 3603.
SAKAGUCHI, M., HU, M., and KEVAN, L., 1990, *J. Phys. Chem.*, **94,** 870.
SAKAGUCHI, M., and KEVAN, L., 1989, *J. phys. Chem.*, **93,** 6039.
THOMPSON, D. H. P., BARRETTE, W. C. JR, and HURST, J. K., 1987, *J. Am. chem. Soc.*, **109,** 2003.